

Quantum walk search based edge detection of images

Pulak Ranjan Giri,* Rei Sato,† and Kazuhiro Saito‡

KDDI Research, Inc., Fujimino-shi, Saitama, Japan

(Dated: October 7, 2025)

Quantum walk has emerged as an essential tool for searching marked vertices on various graphs. Recent advances in the discrete-time quantum walk search algorithm have enabled it to effectively handle multiple marked vertices, expanding its range of applications further. In this article, we propose a novel application of this advanced quantum walk search algorithm for the edge detection of images—a critical task in digital image processing. Given the probabilistic nature of quantum computing, obtaining measurement result with a high success probability is essential alongside faster computation time. Our quantum walk search algorithm demonstrates a high success probability in detecting the image edges compared to the existing quantum edge detection methods and outperforms classical edge detection methods with a quadratically faster speed. A small Qiskit circuit implementation of our method using a one-dimensional quantum walk search has been executed in Qiskit’s *qasm_simulator* and *ibm_sydney(fake)* device.

Keywords: Quantum edge detection, Image processing, Lackadaisical quantum walk, Spatial search

I. INTRODUCTION

Edge detection is a crucial task in digital image processing, with applications across various fields such as medical imaging, forensic science, material science, and traffic surveillance. Many classical edge detection algorithms exist [1–5], but they struggle to keep up with the increasing size and volume of image data. These methods are also extremely time-consuming, as they need to examine each pixel individually to determine the edges. However, in some applications, such as self-driving vehicles [6], real-time fast processing of edge detection is crucial for a safe driving. Quantum computing [7] is considered a promising alternative to efficiently handle large image-datasets faster than the classical methods.

Quantum computing utilizes the properties of quantum mechanics, such as entanglement, superposition, and parallelism, to speed up computational processes. Deutsch’s algorithm to distinguish between constant and balanced functions, Grover’s algorithm [8] and its generalization [9] for searching marked elements in an unsorted database, and Shor’s algorithm [10] for prime factorization are some of the most popular quantum algorithms known for their faster computation times compared to their classical counterparts.

In the context of edge detection, several quantum algorithms, such as QSobel [11] and Hadamard edge detection (HED), [12] exist, that offer exponential speedup over classical methods. These quantum edge detection (QED) algorithms primarily measure pixel gradients to determine the existence of edges. However, they face challenges when the intensity difference between neighboring pixels is small, resulting in low probability amplitudes that are difficult to measure, especially in noisy

conditions. Since quantum computing heavily relies on the probability for successful outcomes, it poses a significant challenge.

In this article, we propose a new quantum edge detection method to address this issue by using a quantum walk search to amplify the amplitudes of edge pixel intensities, making them easier to detect and measure. Our approach involves identifying the edge pixels of a digital image by searching for the edges as a set of marked vertices.

Quantum walk search—a generalization of the Grover’s algorithm, has proven significant for searching on various graphs [13]. In fact, quantum walk (QW), the quantum analog of classical random walk, has become an essential tool for spatial search on graphs. Both the continuous-time and discrete-time quantum walk are extensively employed in the literature [13–19] to search for marked vertices on graphs faster than the random walk. Examples of graphs on which spatial search have been successfully implemented include: n -dimensional square lattice, complete graph, m -partite complete graph, and n -dimensional hypercube among others. Quantum walk exploits quantum superposition to enhance search efficiency, making it a powerful tool for the spacial search on various graph structures.

Many applications of quantum walk leverage their ability to search for the marked vertices faster than their classical counterparts. For instance, a single marked vertex on a two-dimensional grid with N vertices can be found in $\mathcal{O}(\sqrt{N} \log N)$ time [15–17]. Note that, this time complexity is slower by a factor of $\sqrt{\log N}$ compared to the optimal speed of $\mathcal{O}(\sqrt{N})$ achieved by the Grover search. However, a quadratic speedup of $\mathcal{O}(\sqrt{N})$ can be achieved in this grid by adding extra long-range edges to the grid vertices [18, 19].

Searching for the multiple marked vertices, specifically on a two-dimensional grid, is challenging due of the existence of *exceptional configurations* [20–22]. This is a set of specific arrangements of marked vertices that discrete-

* pu-giri@kddi-research.jp

† ei-satou@kddi.com

‡ ku-saitou@kddi.com

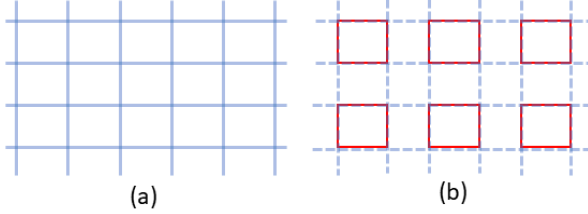


FIG. 1: (a) A two-dimensional lattice of size 4×6 , (b) six 2×2 blocks of the 4×6 two-dimensional lattice.

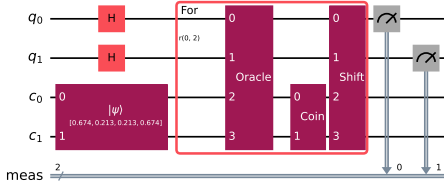


FIG. 2: Qiskit circuit for quantum edge detection with quantum walk search on a cycle with four vertices. Four dimensional coin space, having four basis states: left and right directions and two self-loops with $s = 0.1$, $t = 2$.

time quantum walk search (DTQWS) algorithms with the standard coins cannot find. Recent research on lackadaisical quantum walk [23] shows that modifying the Grover coin operator to flip only the phases of the basis states of marked vertices with attached self-loops can bypass this issue. This modification allows DTQWS to successfully search for the multiple marked vertices in any configuration, including the *exceptional configurations*, with very high success probability, enabling us to successfully exploit it for the quantum edge detection.

This article is organized as follows: A brief discussion on the quantum walk search—an essential tool for our proposed quantum edge detection method, is presented in section II. In section III, a quantum circuit implementation of this detection method has been performed in fake IBM quantum device. Results of the proposed edge detection method are analyzed in section IV. A performance comparison of our edge detection method with other quantum edge detection methods is done in section V and finally we conclude in section VI with a discussion.

II. QW SEARCH ON 2D GRID

Let us assume that the pixel intensities $I(x, y)$ of a $N_1 \times N_2$ digital image are located at the vertices of a $N_1 \times N_2$ rectangular lattice. Fig. 1(a) is an example of a 4×6 two-dimensional lattices. Each vertex has

four regular edges—right(r), left(l), up(u), and down(d). We also add one self-loop at each vertex, so that lackadaisical quantum walk can be implemented on the lattice. Note that, more than one self-loops [17] can also be attached at each vertices for the lackadaisical quantum walk. The vertices are the basis states of the $N = N_1 N_2$ -dimensional Hilbert space, \mathcal{H}_V , and the edges form the $d = 5$ -dimensional Hilbert space, \mathcal{H}_C , of the coin. Quantum walk starts with an initial state, $|\psi_{in}\rangle = |\psi_v\rangle \otimes |\psi_c\rangle$, where

$$|\psi_v\rangle = \frac{1}{\sqrt{N}} \sum_{x=1}^{N_1} \sum_{y=1}^{N_2} |x, y\rangle, \quad (1)$$

is the initial state in the vertex space with (x, y) being the position of the vertices(pixels) and

$$|\psi_c\rangle = \frac{1}{\sqrt{4+s}} (|r\rangle + |l\rangle + |u\rangle + |d\rangle + \sqrt{s}|s\rangle), \quad (2)$$

is the initial state in the coin space, where $|r\rangle, |l\rangle, |u\rangle, |d\rangle$ are the basis states for the right, left, up and down edges respectively. $|s\rangle$ is the basis state for the directed self-loop with weight s .

The time evolution of the initial state, $|\psi_{in}\rangle$, is governed by the unitary operator, $\mathcal{U} = S\mathcal{C}_G$, composed of the modified coin operator, \mathcal{C}_G , followed by the flip-flop shift operator S . Let us assume that the M edge pixels of an image, represented by M vertices, belong to the set \mathcal{T}_M . In the language of quantum walk we have to then find M marked vertices. In this article, we use one-dimensional filter mask [24] to determine the existence of edge pixels. From the horizontal and vertical gradients $I_{h\pm}(x, y)$ and $I_{v\pm}(x, y)$:

$$\begin{aligned} I_{h\pm}(x, y) &= I(x, y) - I(x \pm 1, y), \\ I_{v\pm}(x, y) &= I(x, y) - I(x, y \pm 1), \end{aligned}$$

we can evaluate the existence of edge if the gradient $I_{max}(x, y)$ satisfies the threshold condition

$$I_{max}(x, y) = \max(I_{h+}, I_{h-}, I_{v+}, I_{v-}) \geq a_{th}, \quad (3)$$

where a_{th} is the pre-determined threshold value, that depends on the image. Based on the result in eq. (3), the marking of edges are done by the modified coin operator.

In this article, we are using the following modified coin operator [23]

$$\mathcal{C}_G|x, y\rangle \otimes |s\rangle = \begin{cases} C|x, y\rangle \otimes |b_c\rangle & \text{if } (x, y) \notin \mathcal{T}_M \\ C|x, y\rangle \otimes |b_c\rangle & \text{if } (x, y) \in \mathcal{T}_M; b_c \neq s \\ -C|x, y\rangle \otimes |b_c\rangle & \text{if } (x, y) \in \mathcal{T}_M; b_c = s \end{cases} \quad (4)$$

where $C = 2|\psi_v\rangle\langle\psi_v| - \mathbb{I}_{d \times d}$ is the Grover diffusion operator and b_c is one of the basis states of the coin space. Action of the shift operator on the basis states of the

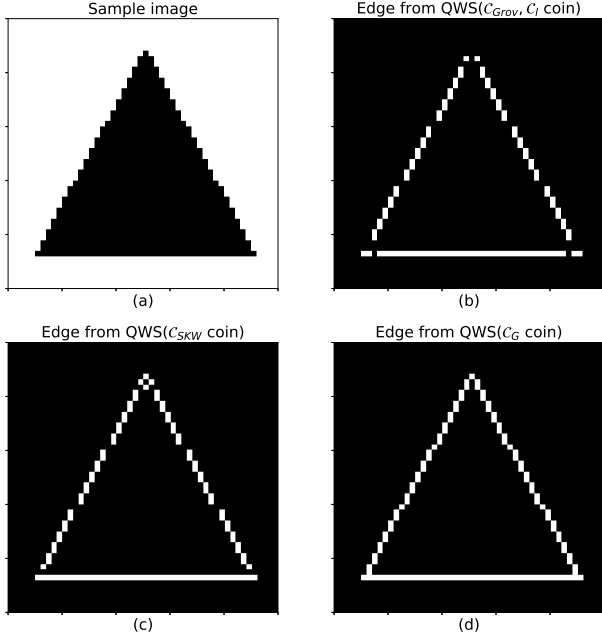


FIG. 3: (a) 50×50 sample image, and its edge detection from quantum walk search algorithm with (b) regular or lackadaisical quantum walk with Grover coin with $s = 0.01$ (c) SKW coin and (d) C_G coin with $s = 0.01$. (b) - (d) are obtained by numerical analysis.

Hilbert space $\mathcal{H} = \mathcal{H}_V \times \mathcal{H}_C$ is summarized as

$$\begin{aligned}
 S|x, y\rangle \otimes |r\rangle &= |x+1, y\rangle \otimes |l\rangle, \\
 S|x, y\rangle \otimes |l\rangle &= |x-1, y\rangle \otimes |r\rangle, \\
 S|x, y\rangle \otimes |u\rangle &= |x, y+1\rangle \otimes |d\rangle, \\
 S|x, y\rangle \otimes |d\rangle &= |x, y-1\rangle \otimes |u\rangle, \\
 S|x, y\rangle \otimes |s\rangle &= |x, y\rangle \otimes |s\rangle.
 \end{aligned} \tag{5}$$

The success probability to find all the M marked vertices(boundary pixels) of the set \mathcal{T}_M , after t time steps, is

$$p_s = \sum_{(x,y) \in \mathcal{T}_M} \sum_{b_c} |\langle x, y | \otimes \langle b_c | \mathcal{U}^t | \psi_{in} \rangle|^2. \tag{6}$$

Measuring the output will give edges of the image. At this present state of quantum computer, it is hard to implement the above discussed 2d DTQWS method in NISQ device for the entire image with a reasonable-size. However, in the next section we instead implement a one-dimensional DTQWS on 2×2 blocks of an image, which requires only four qubits to implement our edge detection method.

III. QUANTUM CIRCUIT IMPLEMENTATION

In this section we implement a Qiskit circuit for the edge detection, which is suitable for deployment in the

current IBM NISQ devices. Because of the limitations of the current NISQ devices, we design a small quantum walk based circuit for our quantum search algorithm with C_G coin on the one-dimensional periodic lattice, which can be exploited for the edge detection of a $N_1 \times N_2$ digital image. Let us assume that the length in both directions N_1 and N_2 are even. If the lengths are not even for a digital image, we can pad appropriately to make them even. Then, we divide the whole image into 2×2 blocks, each having 4 pixels. For example, an 4×6 two-dimensional lattice in fig. 1(a) is divided into six 2×2 red blocks as shown in fig. 1(b). The 4 pixel intensities of each block can be considered as the vertices of a cycle with length $N = 4$. We need two qubits to represent three edges(left, right, self-loop). However, one extra basis state remains which we assign to another self-loop. So, in this model we have two self-loops. Then the Hilbert space for the quantum state is $\mathcal{H}_V \times \mathcal{H}_C = \mathcal{C}^4 \times \mathcal{C}^4$. Because of the various limitations of the current NISQ devices, it is important to keep the number of iterations small, so that the error related to gate noise and decoherence can be minimized. For the present study of the edge detection, we consider a Qiskit circuit with $t = 2$ iterations for the quantum walk search, which is shown in fig. 2. Once the edges of all the 2×2 blocks are evaluated by the quantum circuit, we combine them to obtain the edge of the whole image. Post-processing of the edge information is done with a threshold, a_{th} , to obtain binary edge image. The one-dimensional QWS for the 2×2 blocks of the image to obtain the edge is only done for the **qasm_simulator** and **ibm_sydney(fake)** backend. Rest of the works are based of the two-dimensional QWS of the entire image.

IV. EDGE DETECTION BY DTQWS

One of the important operations in the evolution operator of the DTQWS is the modified coin operator. Several modified coins exist in the literature, such as the Grover coin, C_{Grov} , the coin for the lackadaisical quantum walk search, C_l , SKW coin, C_{SKW} , and the C_G coin. For a detailed discussion on these coins see ref. [23]. It is known that there exist *exceptional configurations* in the search for multiple marked vertices, which can not be found by the C_{Grov} , C_l and C_{SKW} coins. The success probabilities of the marked vertices remain at their initial values in such configurations, despite repeated application of the evolution operator. However, C_G , which has been described in section II, can search any configurations with high success probability. Moreover, it is the only coin which can efficiently search multiple vertices in one-dimensional periodic lattice, which is crucial for the qiskit implementation in section III. A comparison among the results, obtained from the four coins in fig. 2, indicates that C_G is more suitable for edge detection. The 50×50 binary image in fig. 3(a) has three edge-images, 3(b) - 3(d), obtained using the four coins.

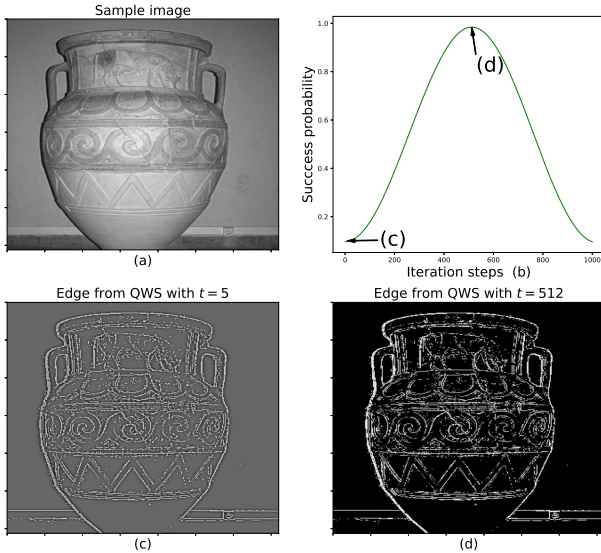


FIG. 4: (a) 360×306 image taken from the BSDS500 database [25], (b) success probability as iteration steps for $s = 0.0001$, edge detected image corresponding to (c) $t = 5$ and $p_s \approx 0.1$ and (d) $t = 512$ and $p_s \approx 0.98$. (b) -(d) are obtained by numerical analysis.

We can see \mathcal{C}_G has detected the edge clearly in fig. 3(d). However, the edges obtained by \mathcal{C}_{Grover} or \mathcal{C}_l coins in fig. 3(b) and by \mathcal{C}_{SKW} coin in fig. 3(c) with 2 iterations have several missing edge pixels. The edge detected by these coins, except \mathcal{C}_G , with iterations corresponding to highest success probability(not shown here) deteriorates even further. In this article, post-processed edge images are binarized with black corresponding to 0 and white corresponding to 1.

Because \mathcal{C}_G is more suitable for searching multiple marked vertices with high success probability, we use this coin for the purpose of edge detection of an image. Usually, the self-loop weight at each vertex of the graph needs to be fixed at an optimum value so that the success probability is maximized and time which corresponds to highest success probability is considered for the edge detection. For example, a sample image in fig. 4(a) has its edge obtained after $t = 5$ iterations in fig. 4(c) and after $t = 512$ iterations in fig. 4(d). As we can see from the curve in fig. 4(b) that the edge in fig. 4(d) corresponds to the maximum success probability, therefore having clear edge compared to fig. 4(c). Finally, in fig. 5, edge detection by our quantum walk search technique has been obtained by three different methods, besides QSobel and Hadamard edge detection. In fig. 5(d) numerical results from the two-dimensional quantum walk search is shown. Then figs. 5(b) and (c) are obtained from the quantum circuit implementation of the edge detection using one-dimensional quantum walk search in section III. The *qasm_simulator* result, shown in fig. 5(b), is better than the result from the noisy *ibm_sydney(fake)* backend, in

fig. 5(c). Figs. 5(e) and 5(f) are obtained with HED and QSobel method respectively. The graphs on the last row of fig. 5, obtained from the raw data of QWS, HED and QSobel methods respectively, show that our method performs better than the other methods.

V. PERFORMANCE COMPARISON

In this section, performance of our quantum edge detection model over other significant quantum edge detection models, specifically Hadamard edge detection and QSobel model, is discussed. Our model demonstrates a markedly high total success probability, $p_s \approx 1$, outperforming other models. The success probability for M edge vertices/targets of a digital image with N pixels can be optimized by tuning the self-loop parameter s accordingly. Usually, s and t , corresponding to the optimized p_s , depend on N, M , and the dimension of the lattice. A detailed numerical analysis of how the total success probability p_s behaves as a function of the self-loop weight s is studied in ref. [23]. Although a formal expression for the scaling of p_s as a function of N and M is not known, the study further shows that even with a suitably chosen fixed s the success probability p_s remains reasonably high over a wide range of N and M , as can be seen from figs. 3(b) and 5(b) of ref. [23]. Generally, the lower the value of s , the higher the success probability p_s and time t , as can be seen from figs. 2(1d case) and fig. 4(2d case) of ref. [23].

In the case of Hadamard edge detection (HED) method, the encoding of pixel intensities of a $\sqrt{N} \times \sqrt{N}$ image is done into the normalized amplitudes of a quantum state of the form

$$|\psi_{in}\rangle = \sum_{i=0}^{2^{2n}-1} c_i |i\rangle, \quad (7)$$

where amplitudes, c_i s, are obtained by concatenating and normalizing all the rows of the image's pixel intensities. This encoding method is referred to as quantum probability image encoding [26]. Here, $2^{2n} = N$ represents the total number of pixels in the image. The process involves applying a Hadamard gate to the first qubit of the encoded state in eq. (7), which gives

$$|\psi_f\rangle = \frac{1}{\sqrt{2}} \sum_{i=0}^{2^{2n}-1-1} (c_{2i} + c_{2i+1}) |2i\rangle + (c_{2i} - c_{2i+1}) |2i+1\rangle, \quad (8)$$

where only odd basis states encode the edge information, while all the even basis states are not useful for edge detection purposes. An edge is identified at position $(2i+1)$ if the gradient/amplitude meets a threshold condition, specifically $(c_{2i} - c_{2i+1}) \geq a_{th}$. The gradients obtained in eq. (8) are $(c_0 - c_1), (c_2 - c_3), \dots$. The remaining gradients/edges, such as $(c_1 - c_2), (c_3 - c_4), \dots$, can be

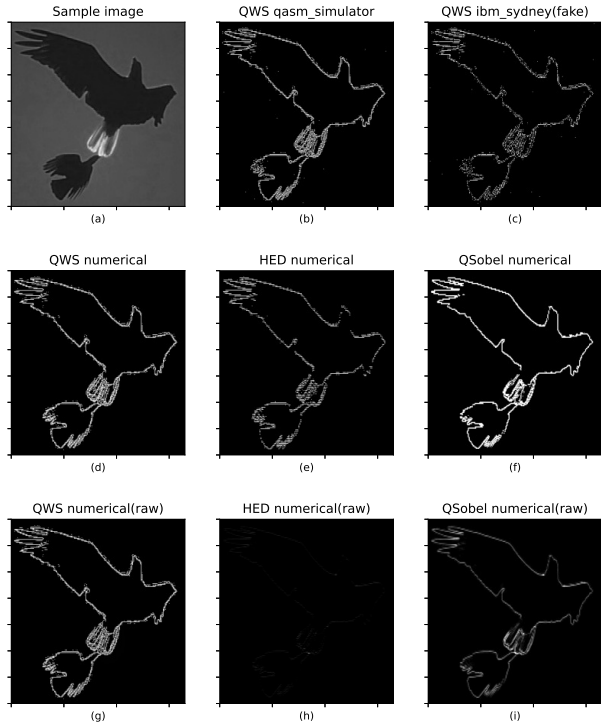


FIG. 5: A sample (a) 330×350 image from **BSDS500** database [25] is used to obtain its edge from Qiskit circuit for the 2×2 blocks of the image with (b) `qasm_simulator`(no noise), $\bar{p}_s \approx 0.53$ and (c) `ibm_sydney(fake)` backend, $\bar{p}_s \approx 0.40$, $s = 0.1$, $t = 2$. Also edge obtained with the two-dimensional numerical QWS of the 330×350 image with (d) QWS with $s = 0.0001$, $t = 791$, $p_s \approx 0.98$, (e) HED, $\bar{p}_h \approx 0.0031$, (f) QSobel, $p_q \approx 0.0095$. Edge obtained with raw the data(without post-processing) obtained from numerical analysis of the entire image with (g) QWS with $s = 0.0001$, $t = 791$, $p_s \approx 0.98$, (h) HED, $\bar{p}_h \approx 0.0031$, (i) QSobel, $p_q \approx 0.0095$.

obtained by applying a shift operation to the initial state in eq. (7) and then continuing with the subsequent steps. The total success probability for detecting edges is constrained by the limits

$$\begin{aligned} p_h &= \sum \left| \frac{1}{\sqrt{2}} (c_{2i} - c_{2i+1}) \right|^2 \leq 1/2 \\ \tilde{p}_h &= \sum \left| \frac{1}{\sqrt{2}} (c_{2i+1} - c_{2i+2}) \right|^2 \leq 1/2. \end{aligned} \quad (9)$$

More than $1/2$ of the success probability is lost with the discarded even basis states. As a result, the total success probability for the edge detection using this model is limited to $p_h \leq 1/2$.

In QSobel, the initial state is of the form [11]

$$|\psi_{in}\rangle = \frac{1}{\sqrt{N}} \sum_{x=0}^{2^n-1} \sum_{y=0}^{2^n-1} |0\rangle^{\otimes 9} |C_{xy}\rangle |x, y\rangle, \quad (10)$$

where intensity of image's pixel is encoded in the angle of the color qubit $|C_{xy}\rangle = \cos \theta_{xy} |0\rangle + \sin \theta_{xy} |1\rangle$. The final state, which contains the edge information, is

$$|\psi_f\rangle = \frac{1}{\sqrt{N}} \sum_{x=0}^{2^n-1} \sum_{y=0}^{2^n-1} |\Omega_{xy}\rangle |x, y\rangle, \quad (11)$$

where qubit $|\Omega_{xy}\rangle$ contains the color information of the edge. The total success probability to measure M edge pixels can be bounded as

$$p_q = M/N, \quad (12)$$

which is much less than the success probability of our edge detection model for $M \ll N$. The actual success probability $p_q = \sum_{(x,y) \in \mathcal{T}_M} \sin^2 \theta_{xy}/N$ is even smaller than the upper bound M/N obtained in eq. (12).

The effect of higher success probability on edge detection can be understood from the image edges presented in the third row of fig. 5, which are obtained from the raw data(without post-processing). Numerical values of all the success probabilities are obtained from the raw data. Note that, the success probability of our model $p_s \approx 0.98$ is much higher than the success probabilities $\bar{p}_h = (p_h + \tilde{p}_h)/2 \approx 0.0031$ (HED), and $p_q \approx 0.0095$ (QSobel) respectively. Since our model has high success probability, the raw data plot in fig. 5(g) is almost same as its post-processed data plot in fig. 5(d). Whereas, for HED and QSobel cases edges obtained from the raw data plots in figs. 5(h) and 5(i) respectively are very weak compared to their post-processed plots in figs. 5(e) and 5(f). In Qiskit circuit simulation, the success probability is for the 2×2 blocks only. So, we have obtained the average success probability over all the blocks present in the image. Note that, because of the noise and other errors, the average success probability $\bar{p}_s \approx 0.40$ for `ibm_sydney(fake)` is less than the success probability $\bar{p}_s \approx 0.53$ for the `qasm_simulator`(no noise). We iterated for $t = 2$ in the Qiskit circuit because of the limitations of the simulator. However, in the pure numerical analysis of the one-dimensional quantum walk search for the 2×2 block, a much higher success probability can be achieved.

VI. CONCLUSIONS

In this article, we proposed a quantum walk search method for the edge detection of digital images. Existing quantum methods for the edge detection often struggle with low success probability, especially in noisy environments. Our approach, which utilizes quantum walk search, boasts a higher success probability, $p_s \gg p_h, p_q$, compared to other quantum edge detection models discussed in this article, making it more robust. We have implemented a small quantum circuit using Qiskit that can run on the IBM quantum computer; however, a full quantum advantage requires a quantum circuit for the entire $N_1 \times N_2$ image in 2d, which current NISQ quantum

computers cannot handle. Nonetheless, because quantum walk search is faster than exhaustive search, our method outperforms classical edge detection methods in terms of speed.

The presence of noise in the **ibm_sydney**(fake) simulator adversely affect the edge detection with reduced success probability as can be seen from fig. 5(c). In our study, we have not considered the presence of noise in the sample images. However, the presence of noise in the sample images should not impact the success probability of the image edge of our model assuming the oracle can mark the target vertices/edges accurately. Because, unlike other quantum edge detection models, the initial state of our model $|\psi_{in}\rangle = |\psi_v\rangle \otimes |\psi_c\rangle$ is the equal superposition of all the vertex states, which is independent of whether the sample image has noise or not.

For future work, it would be worthwhile to explore the impact of error mitigations on the quantum walk search method for our edge detection. Additionally, analyzing the Qiskit implementation of this edge detection method using quantum walk search in 2-dimensional grid, as presented in section II, and its deployment on real quantum devices would be interesting.

Data availability Statement: The data and database information generated during and/or analyzed during the current study are included in the article.

Conflict of interest: The authors have no competing interests to declare that are relevant to the content of this article.

[1] L. Sobel, Stanford Univ Press, (1970).
 [2] J. Prewitt, New York: Picture Process and Psychopictoric Press, 75–149, (1970).
 [3] R.A. Kirsch, Comput Biol Med, 18, 113–125, (1971).
 [4] J. Canny, IEEE TPAMI, 8, 679–697, (1986).
 [5] J. M. Niya, A. Aghagolzadeh, Proceedings of the 12th IEEE Mediterranean Electrotechnical Conference, Ajaccio, 1, 281–284, (2004).
 [6] P. Quoc Thai, H. Duc Tri, B. Van Ga and P. Van Binh, Proc. 2022 7th National Scientific Conference on Applying New Technology in Green Buildings (ATiGB), pp. 225-228, Oct. (2022).
 [7] M. Nielsen and I. Chuang, *Quantum Computation and Quantum Information* (Cambridge University Press, Cambridge, 2000).
 [8] L. K. Grover, Pro. 28th Annual ACM Symp. Theor. Comput. (STOC) **212** (1996).
 [9] P. R. Giri and V. E. Korepin, Quant. Inf. Process. **16** 1-36 (2017).
 [10] P. W. Shor, Polynomial-time algorithms for prime factorization and discrete logarithms on a quantum computer, Proc: 35th Annual Symposium on Foundations of Computer Science, Santa Fe, NM, 20-22, Nov. (1994).
 [11] Y. Zhang, K. Lu, and Y. Gao, Sci. China Inf. Sci. 58, 1-13 (2015).
 [12] Xi-Wei Yao et al. Phys. Rev. X (2017).
 [13] R. Portugal, *Quantum Walks and Search Algorithms*, Springer, New York (2013).
 [14] A. M. Childs and J. Goldstone, Phys. Rev. A **70** 022314 (2004).
 [15] A. Tulsi, Phys. Rev. A **78** 012310 (2008).
 [16] A. Ambainis, A. Bačkurs, N. Nahimovs, R. Ozols and A. Rivosh, Proceedings 7th Annual Conference Theory of Quantum Computation, Communication, and Cryptography, TQC 2012, 87–97. Springer, Tokyo (2013).
 [17] T. G. Wong, J. Phys. A Math. Theor. **48** 43, 435304 (2015).
 [18] P. R. Giri, Int. J. Theor. Phys. 62, 121 (2023).
 [19] T. Osada, K. Sanaka, W. J. Munro, and K. Nemoto, Phys. Rev. A 97, 062319 (2018).
 [20] N. Nahimovs and A. Rivosh, Proceedings of the 10th International Doctoral Workshop on Mathematical and Engineering Methods in Computer Science, MEMICS 2015 (Springer, Telč, Czech Republic, 2016) pp. 79-92.
 [21] A. Ambainis, A. Rivosh, Proceedings of SOFSEM'08, 485-496, (2008).
 [22] M. Li and Y. Shang, New J. Phys. 22 123030 (2020).
 [23] P. R. Giri, Eur. Phys. J. D 77, 175 (2023).
 [24] A. Geng, A. Moghiseh, C. Redenbach, and K. Schladitz, Quantum Mach. Intell. 4, 15 (2022).
 [25] David Martin, Charless Fowlkes, Doron Tal, and Jitendra Malik. A database of human segmented natural images and its application to evaluating segmentation algorithms and measuring ecological statistics. In International Conference on Computer Vision, volume 2, pages 416–423. IEEE, (2001).
 [26] G. Cavalieri, and D. Maio, arXiv:2012.11036 [quant-ph].